GEOPHYSICS, VOL. 56, NO. 1 (JANUARY 1991); P. 80–89, 8 FIGS.

Robust polynomial fitting method for regional gravity estimation

J. F. Beltrão*, J. B. C. Silva*, and J. C. Costa*

ABSTRACT

Standard polynomial fitting methods are inconsistent in their formulation. The regional field is approximated by a polynomial fitted to the *observed field*. As a result, in addition to the nonuniqueness in the definition of the regional field, the fitted polynomial is strongly influenced by the residual field (observed field minus regional field). We present a regional-residual separation method for gravity data which uses a robust procedure to determine the coefficients of a polynomial fitted to the observations. Under the hypothesis that the regional can be modeled correctly by the polynomial surface, the proposed method minimizes the influence of the residual field in the fitted surface.

The proposed method was applied to real gravity data from Ceará state, Brazil, and produced information on zones of possible crustal thickening and the occurrence of lower-crustal granulitic rocks thrust into the shallow subsurface.

INTRODUCTION

The gravity field is produced generally by the superposition of overlapping gravitational effects of many sources, whose individual anomalies may be difficult to isolate. The terms "residual" and "regional" commonly are used to differentiate between anomalies from local, near surface masses and those arising from larger and generally deeper features, respectively. In many cases, the choice of regional depends on the residual anomalies targeted for interpretation. There are many methods to separate the regional field from the gravity field. According to Nettleton (1976), regional-residual techniques in the analysis of potential field data may be grouped into graphical, spectral, and polynomial fitting methods.

The graphical method is slow and cannot be automated. The only constraint imposed on the regional field, besides the interpreter's intuition, is the smoothness. As a result, there will be several solutions to the separation problem, and the inherent subjectivity may be either an advantage or a drawback depending on the interpreter's experience and ability to incorporate relevant geologic information about the regional field (Skeels, 1967; Gupta and Ramani, 1980).

Spectral methods, on the other hand, provide more quantitative means to characterize the smoothness of a regional field, namely, by its predominantly low-frequency spectral content. They are faster and less subjective than the graphical method because the separation is performed by filtering the total field with a suitable low-pass filter. In applying spectral methods, regional fields may be assumed to be produced either by wide or deep-seated sources. However, due to the overlap of the regional and residual spectra, a complete separation is not possible and two kinds of errors, signal distortion and noise transmission, are always present. Signal distortion is the elimination of part of the signal spectral content by a filtering operation. Noise transmission is the incomplete removal of the noise by a filtering procedure. The total sum of these two errors can be minimized by using a Wiener filter, as shown by Jacobsen (1987). However, any spectral method which assigns null spectral content to the zero frequency in the residual (and this is the rule) will produce residuals contaminated by pseudoanomalies (Ulrych, 1968). These pseudoanomalies have the opposite sign from the real residual anomaly. They arise because assigning a null spectral content to the residual zero frequency is equivalent to obtaining a residual with a null spatial mean. In other words, there must always be residual anomalies of both signs even though the real residual anomaly may be of just one sign.

Polynomial fitting methods assume that a polynomial surface adequately models the regional field whose smoothness is controlled by the polynomial order (Agocs, 1951; Simpson, 1954). Since the polynomial is fitted to the total field, any attempt to model a complex regional by a high-order polynomial will produce an effect similar to the noise transmission of spectral methods. Accordingly, a very low-

Manuscript received by the Editor August 14, 1989; revised manuscript received July 9, 1990.
*Centro de Geociencias, Univêrsidade Federal do Para, Caixa Postal 1611, 66000 Belém, Pará, Brazil.

order polynomial may not be sufficient to model a smooth but irregular field and an effect similar to signal distortion will appear. The fitting polynomial usually includes a constant term, and because the least-squares method is commonly employed, the sum of the residuals is always zero. This implies the presence of both positive and negative residuals. Since a gravity anomaly over a simple body is commonly of one sign, in this case the least-squares method will produce pseudoanomalies with the opposite sign from the true anomaly. A procedure to select the "optimum" polynomial order, based on the correlation between residuals of successive orders, is presented by Abdelrahmam et al. (1985).

The presence of undesirable pseudoanomalies in the residuals has been pointed out by many authors (Agocs, 1951; Paul, 1967; Skeels, 1967; Rao et al., 1975); however, little has been done to lessen their influence. Skeels (1967) recommends graphical separation, so that pseudoanomalies can be deliberately avoided. El-Bathroukh and Zentani (1980) simply add a constant base level to the fitted regional in order to produce essentially positive residual anomalies. This procedure was supported by geologic evidence of shallow structures with strictly positive density contrast. Rao et al. (1975) present a polynomial fitting method where the polynomial coefficients are updated iteratively. At each iteration a polynomial is fitted to the regional approximated by the difference between the observed field and a "revised" residual, defined as the central positive part of the residual (for a positive density contrast) obtained at the previous iteration. The negative and positive halo of pseudoanomalies surrounding the main positive residual is not included in the "revised" residual. To detect the pseudoanomalies automatically, however, the area should enclose just one true residual anomaly.

In this paper we present a regional-residual separation method based on polynomial fitting in which the coefficients are determined by a robust procedure consisting of iteratively reweighted least-squares solutions. By successively assigning small weights to large residuals, their influence in the fitted regional is minimized, regardless of the "true" residual anomalies signs. Moreover, the minimization of the residual influence is equivalent to the assumption that local anomalies due to isolated bodies have gravity values of the same sign. As a result, high-order polynomials may be employed, further reducing the signal distortion. In contrast with the method presented by Rao et al. (1975), the proposed method can *automatically* detect and eliminate the pseudoanomalies even in a complex area containing several residual anomalies.

METHODOLOGY

The definition of a data fitting method requires the specification of an objective function and a decision-making criterion (Gol'tsman, 1977). In the least-squares method, the objective function is the sum of the squared differences between each observation and the value of the fitting functional at that observation point. The decision-making criterion is the minimization of the objective function. A general, robust M estimator (Huber, 1981) can be obtained by minimizing the objective function

$$Q(\mathbf{c}) = \sum_{i=1}^{N} u(r_i/s), \tag{1}$$

where u is a functional defining the particular robust method and r_i is the residual at the ith observation, given by

$$r_i = g_i^0 - f(x_i, y_i, z_i, \mathbf{c}). \tag{2}$$

g_i^0 is the ith observation, $f(x_i, y_i, z_i, \mathbf{c})$ is the fitting functional evaluated at the ith observation point (x_i, y_i, z_i), $\mathbf{c}$ is a set of parameters uniquely defining the functional f, and s is a scale factor. The least-squares method can be viewed as an M estimator with $u(v) = v^2$.

Regional-residual separation by polynomial fitting assumes that the regional may be fitted by a complete nth-order polynomial in both x and y directions, that is,

$$f(x, y, z, \mathbf{c}) = P_n(x, y, \mathbf{c}), \tag{3}$$

where $\mathbf{c}$ is the set of polynomial coefficients.

Of necessity, the polynomial is fitted to the total field and not to the (unknown) regional by the least-squares method (Agocs 1951; Simpson Jr., 1954; Abdelrahman et al., 1985). As a result, high-order polynomials will fit part of the residual. Computed residuals in this case will have smaller amplitudes than true residuals. Moreover, spurious negative residuals will show up because the fitting of a function having a constant term (the base level) by the least-squares method requires that the sum of residuals be zero. These difficulties can be reduced by using fitting methods more robust than least-squares in the class of M estimators described above. Any M estimator which uses a function $u(v)$ in equation (1) increasing less rapidly than v^2 is more robust than least squares.

The necessary condition for the existence of a minimum of the objective function $Q(\mathbf{c})$, defined in equation (1) is

$$\sum_{i=1}^{N} q(r_i/s) \frac{\partial}{\partial c_j} f(x, y, z, \mathbf{c}) \Bigg|_{\substack{x=x_i \\ y=y_i \\ z=z_i}} = 0, \quad j = 1, 2, \ldots M, \tag{4}$$

where

$$q(r_i/s) = \frac{\partial u}{\partial r}\Bigg|_{r=r_i}.$$

Substituting equation (3) in equation (4) and using matrix notation

$$\underline{\mathbf{A}}^T\mathbf{q} = \mathbf{0}, \tag{5}$$

where $\underline{\mathbf{A}}$ is an $N \times M$ matrix whose a_{ij} element is

$$a_{ij} = \frac{\partial}{\partial c_j} P_n(x, y, \mathbf{c})\Big|_{\substack{x=x_i \\ y=y_i}},$$

and $\mathbf{0}$ is the null vector.

Writing

$$\mathbf{q} = \underline{\mathbf{W}}\mathbf{r}, \tag{6}$$

where $\underline{\mathbf{W}}$ is an $N \times N$ diagonal weighting matrix, whose ith element is given by

$$w_i = q_i/r_i, \tag{7}$$

with $q_i = q(r_i/s)$ and, substituting equation (6) in equation (5),

$$\underline{\mathbf{A}}^T\underline{\mathbf{W}}\mathbf{r} = \mathbf{0}. \tag{8}$$

Because the functional f is linear in $\mathbf{c}$, the residual vector may be written as

$$\mathbf{r} = \mathbf{g}^0 - \underline{\mathbf{A}}\mathbf{c}, \tag{9}$$

where $\mathbf{g}^0$ is the vector of observations. Substituting equation (9) in equation (8),

$$\underline{\mathbf{A}}^T\underline{\mathbf{W}}\underline{\mathbf{A}}\mathbf{c} = \underline{\mathbf{A}}^T\underline{\mathbf{W}}\mathbf{g}^0. \tag{10}$$

Because $\underline{\mathbf{W}}$ depends implicitly on $\mathbf{c}$, equation (10) cannot be solved directly for vector $\mathbf{c}$. Instead, it is solved iteratively combining equations (9) and (10). At the kth iteration, the weighting matrix $\underline{\mathbf{W}}^{(k)}$ is obtained from $\mathbf{c}^{(k)}$, the kth approximation of $\mathbf{c}$, using equations (7) and (9). The $(k + 1)$st approximation of $\mathbf{c}$ is obtained from equation (10):

$$\mathbf{c}^{(k+1)} = [\underline{\mathbf{A}}^T\underline{\mathbf{W}}^{(k)}\underline{\mathbf{A}}]^{-1}\underline{\mathbf{A}}^T\underline{\mathbf{W}}^{(k)}\mathbf{g}^0. \tag{11}$$

The iteration starts with $\underline{\mathbf{W}}^{(0)} = \underline{\mathbf{I}}$, the identity matrix (corresponding to ordinary least squares) and stops when the median of the absolute value of the residuals is stabilized because at this stage the residuals will have little influence on the fitted function.

Since u, q_i, and w_i are interrelated, it may be simpler to specify w_i directly as a function of r_i, instead of u as a function of r_i, as shown in the next section.

APPLICATION TO SYNTHETIC DATA

To evaluate the performance of the proposed method, it was applied to the gravity field produced by combinations of adjacent vertical prisms simulating shallow and deep sources. The shallow bodies model intracrustal bodies having a density contrast of 200 kg/m^3 and depth to the top between 10 and 15 km, with a thickness of 2.5 km. The deep sources simulate the crust-mantle interface with a density contrast of 400 kg/m^3, and depth to the top between 27.5 and 30.0 km.

Regional-residual separation by polynomial fitting commonly assumes that the regional field is a first, second, or third order polynomial (Rao et al., 1975; Abdelrahman et al., 1985). Common geologic structures, however, produce complex regional fields, so that the distortions in the calculated regional are worse than those usually reported from tests using synthetic data. To illustrate this point, we fitted the data shown in Figure 1a by polynomials of orders 3, 5, 7, and 9 using the least-squares method. The results are shown in Figures 1c through 1f, respectively. Figure 1a combines a regional field (Figure 1b) and a residual field consisting of positive and negative anomalies, corrupted with Gaussian noise having a standard deviation of 0.3 mGal. The shape of the fitted regional starts to approximate the shape of the true regional for a polynomial of order 5, but at the same time the presence of the residual in the fitted regional appears. This example shows that even the field of a simple feature such as a smooth warping of the interface crust-mantle cannot be satisfactorily modeled by a third-order polynomial. Moreover, discontinuities of the crust-mantle interface are expected to be more complex than the one employed to simulate the regional field of Figure 1b (Browne et al., 1985; Ritz and Robineau, 1986; Galson and Mueller, 1986).

In the following tests we used a robust procedure in which the weighting matrix in equation (11) is

$$w_i = \exp\ -[0.6745\ r_i^{(k-1)}/s^{(k-1)}]^2, \tag{12}$$

where $s^{(k-1)}$ is the median of the absolute values of the residuals at the $(k - 1)$st iteration, and the constant 0.6745 made $s^{(k-1)}$ a consistent estimator of the standard deviation in the case of observations contaminated by Gaussian noise (Anderson, 1982). Figure 2a shows the normalized weight w as a function of the absolute value of the residual for the least-squares method and proposed robust procedure. The

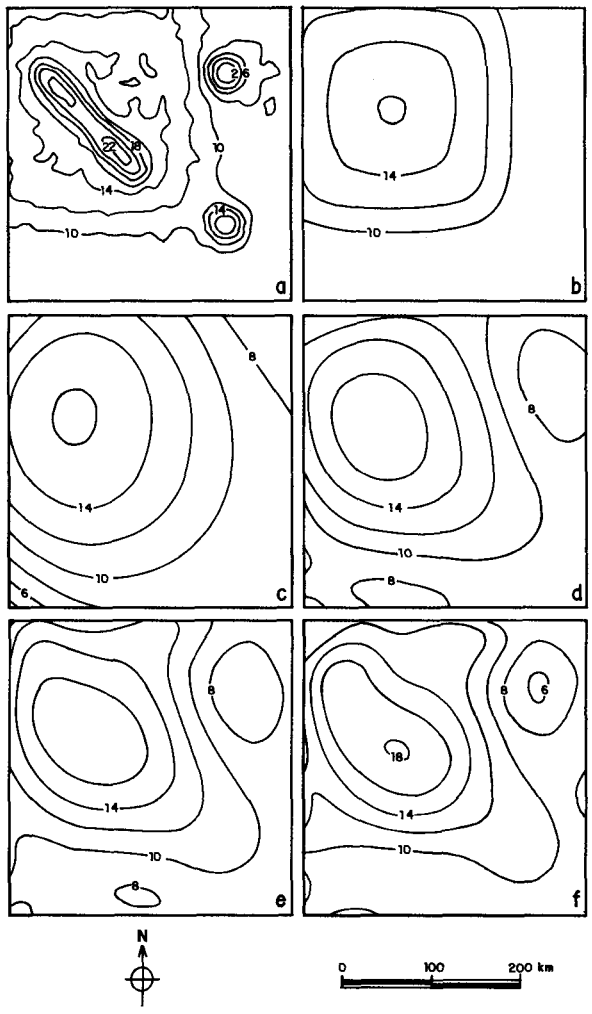

FIG. 1. Least-squares polynomial fitting of the total field (a) composed of a simulated regional field caused by a single deep prism (shown in b) and a simulated residual field due to shallow sources and random noise. Polynomial orders 3 (c), 5 (d), 7 (e), and 9 (f) were employed to extract the regional. Contour interval is 2 mGal.

weight normalization allows better comparison between the methods without affecting the behavior of the individual methods because only the relative weights matter. In the least-squares method, every observation is assigned the same degree of importance regardless of the residual value it produces. The robust procedure, on the other hand, attributes importance only to observations producing small residual values. Observations containing a high percentage of any residual field are virtually excluded from the fitting process.

Tests using the weights of equation (12) produced much better results than least squares. However, pseudo-anomalies persisted in the residual map and the amplitudes of the residual anomalies were smaller than the true values. These distortions happened because in the iterative process an observation producing an initially high residual is assigned a small weight in the regional fitting process, producing a still higher residual, and so on. Because the selected weighting function decreases so rapidly with increasing residual values and especially because it has a lower limit (zero), residual enhancement is prematurely halted. For example, observations producing residuals with absolute values of 1.5 and 2.0 are assigned weights of about 7.71×10^{-8} and 2.26×10^{-13}, respectively. Although these two weights differ by five orders of magnitude, they are effectively zero compared with weights close to unity assigned to observations producing very small residuals.

To reduce the amplitude distortion, we used weights defined as

$$w_i^{(k)} = e^{-t^2}, \qquad t < 5.48, \tag{13a}$$

and

$$w_i^{(k)} = -A\left(\frac{t - 5.48}{r_{\mathrm{MAX}}}\right)^2, \qquad t \geq 5.48, \tag{13b}$$

where

$$t = \frac{0.6745\, r_i^{(k-1)}}{s^{(k-1)}},$$

r_{MAX} is the maximum absolute value of the residuals at the $(k-1)$st iteration, and A is an amplitude factor set equal to 0.1. The threshold of 5.48 was chosen because it corresponds to virtually null weights in equation (13a). The weights defined in equations (13a) and (13b) were applied to a variety of separation problems using synthetic data. Several combinations of 2-D and 3-D regional and residual fields were employed to simulate different geologic settings, producing similar results, so that these weights may be considered appropriate for general use.

Figure 2b compares the weights defined by equations (13a) and (13b) for a typical value of 0.23 for s with the weights employed in the least-squares method. Observations producing residuals greater than 1.85 will be assigned a negative weight, that is, they will "push" the regional surface instead of "pulling" it. The use of negative weights in data fitting is rather uncommon and, to the authors' knowledge, has only been suggested by Tukey (1965).

Henceforth, we refer to the robust method using the strictly positive weights of equation (12) as PW and the one using both positive and negative weights of equations (13a) and (13b) as PNW.

In the following tests, the result obtained upon convergence of the PW method is used as an initial guess for the iteration using the PNW method. Since the negative weights have no lower limit, the iteration will eventually assign high negative weights to all observations. Since only the relative weights are important, this situation is equivalent to ordinary least squares. At this point, the residuals will be small and the process will start to behave mostly as PW again. The

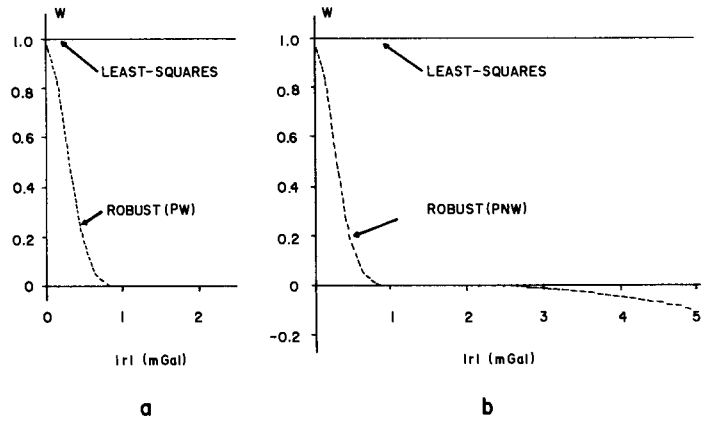

FIG. 2. Normalized weights as a function of the residual for the least-squares and the proposed method using (a) strictly positive weights (PW), and (b) both positive and negative weights (PNW).

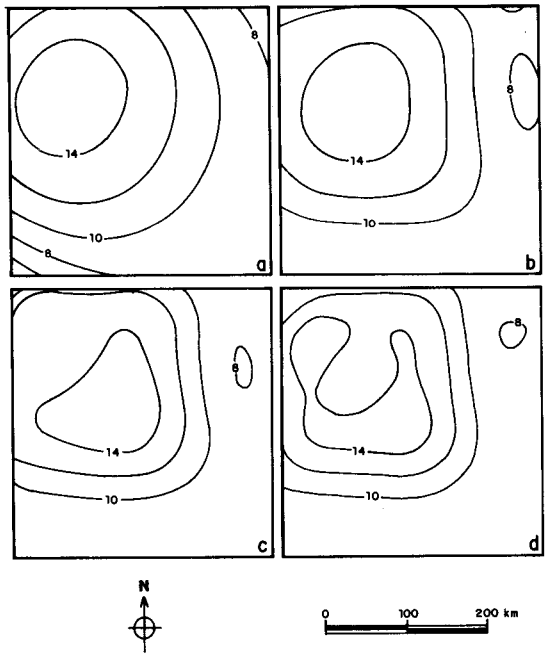

FIG. 3. Polynomial fitting of the gravity field shown in Figure 1a using the PNW method. Polynomial orders 3 (a), 5 (b), 7 (c), and 9 (d) were employed to extract the regional. Contour interval is 2 mGal.

median of the absolute residuals will, therefore, oscillate during the iterations; consequently, a stopping criterion different from the one described for PW must be adopted. The PNW iterative process is interrupted at the kth iteration where one of the following conditions is met: (a) the ratio between the maximum residuals at the $(k + 1)$st and kth iteration is greater than 1.3; or (b) the median of the absolute value of the residuals increases along three successive iterations starting with the kth iteration.

For comparison, the PNW method was applied to the gravity field of Figure 1a assuming polynomials of orders 3, 5, 7, and 9. The results are shown in Figures 3a through 3d. Comparing Figures 1 and 3, we see that the PNW method produces regional fields closer to the true field (Figure 1b), regardless of the assumed polynomial order. In addition, regionals of orders 5, 7, and 9 differ only slightly. In contrast, the corresponding regionals extracted with the least-squares method contain considerable differences. This test shows that the choice of the polynomial order is much less critical in the PNW method than in the least-squares method.

The next test illustrates that the proposed PNW method produces reasonable results not only in modeling simple regional field as the one shown in Figure 1b, but also in separating complex two-dimensional (2-D) regional fields. For comparison, we also present the results using ordinary least squares, the PW robust method, the fitting of orthogonal polynomials (Ralston and Rabinowitz, 1978), and the spectral method of Syberg (1972).

Figure 4a shows the total (regional plus residual) gravity anomaly corrupted with additive, zero-mean Gaussian noise having a standard deviation of 0.3 mGal. Figures 4b and 5a show the theoretical regional and residual fields, respectively. The regional field was modeled by a polynomial of order 9 by the least-squares, PW, and PNW methods and the results are shown in Figures 4c, 4d, and 4e, respectively. The order of the polynomial surface is primarily dictated by

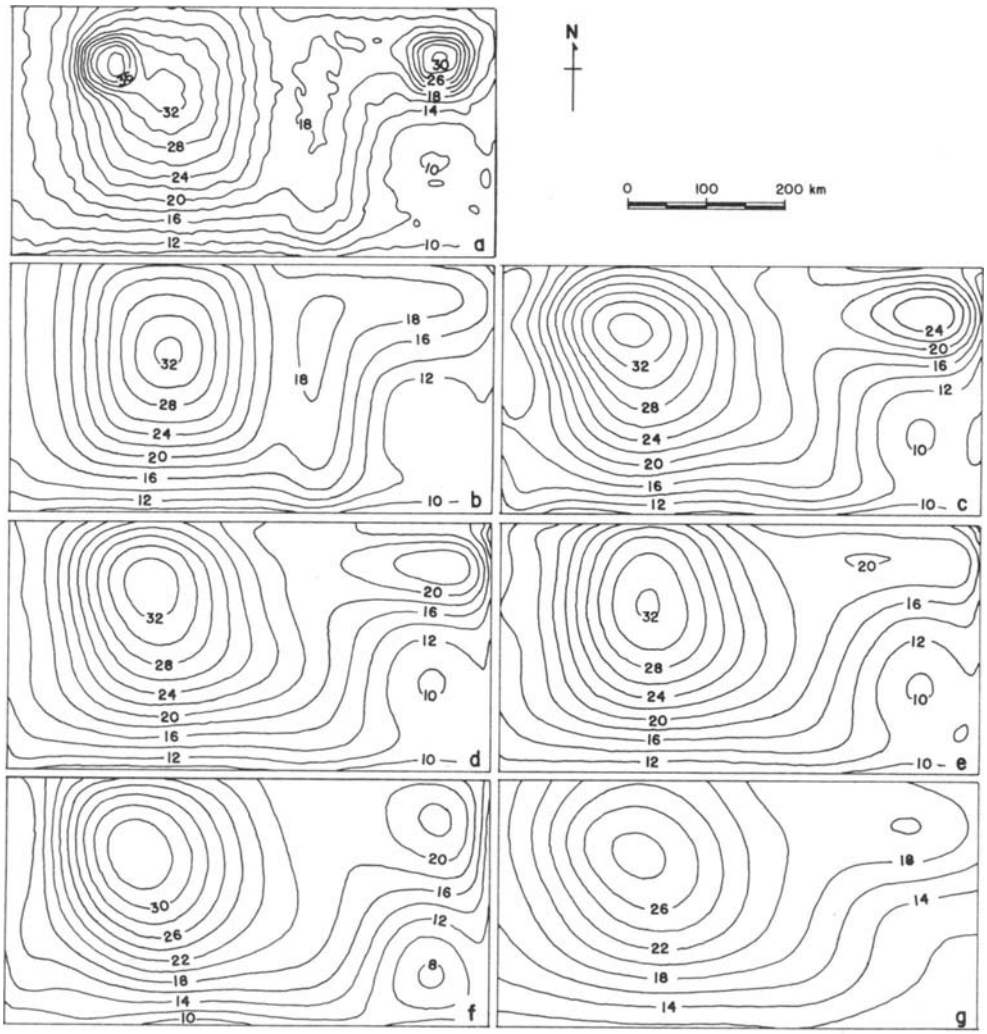

FIG. 4. Comparison among regionals obtained by different separation methods applied to the total field (a) composed of a theoretical regional (shown in b), a residual (Figure 5a), and random noise. (c) Least-squares, (d) PW, (e) PNW, (f) orthogonal polynomials of orders 4 (north-south) and 9 (east-west), and (g) spectral method. Contour interval is 2 mGal.

the amount of desired detail in the regional field. A very high-order polynomial tends to fit the observations exactly and may not detect the residuals. Also, the computation of coefficients of the high-order terms is affected by the finite precision of computer arithmetic. A practical limit on the polynomial order is therefore attained when regionals of successive orders do not change appreciably.

The regional field produced by the least-squares method (Figure 4c) is severely distorted in the vicinity of the northeastern and northwestern corners due to the incorporation of the two residual anomalies in the fitted surface. At the northeastern corner, this distortion is shown by the presence of a large spurious anomaly. At the northwestern corner, the presence of the residual anomaly in the regional does not produce an isolated anomaly because of the presence of the large regional anomaly. However, a local distortion in the gradient gives rise to a false northwest-southeast trend in the main computed regional anomaly.

On the other hand, the regional field obtained by the PW method exhibits a smaller influence of the residual anomalies, denoted by the smaller amplitude of the pseudoanomaly at the northeastern corner and by a smoother gradient at the northwestern corner. However, the PNW method produces a fitted regional field closest to the true one (Figure 4e). The main distortion, in the middle-eastern portion, is probably due to the low order of the fitting polynomial. The fitted ninth-order polynomial surface cannot account for fine details in the theoretical regional such as the 40 km wide low in the middle-eastern portion, elongated in the north-south direction.

Figure 4f shows the computed regional using an orthogonal polynomial with orders 4 and 9 in the north-south and east-west directions, respectively. In general, it is slightly better than the least-squares method using a nonorthogonal polynomial of order 9, regarding the influence of both residual anomalies. The linear east-west feature in the northeastern corner of the true regional is, however, poorly defined. Moreover, a large, spurious low is introduced in the southeastern corner.

Figure 4g displays the regional field obtained by the spectral method of Syberg (1972). It defines only general, smoothed features of the true regional with a substantial distortion in the gradient, shape, and amplitude of the anomalies.

The residuals, obtained by subtracting from the total field (Figure 4a) the regionals corresponding to the above described methods, are shown in Figures 5b through 5f. In the least-squares case (Figure 5b), both residual anomalies show a considerable loss of amplitude. There are spurious negative anomalies at their eastern and western borders. More-

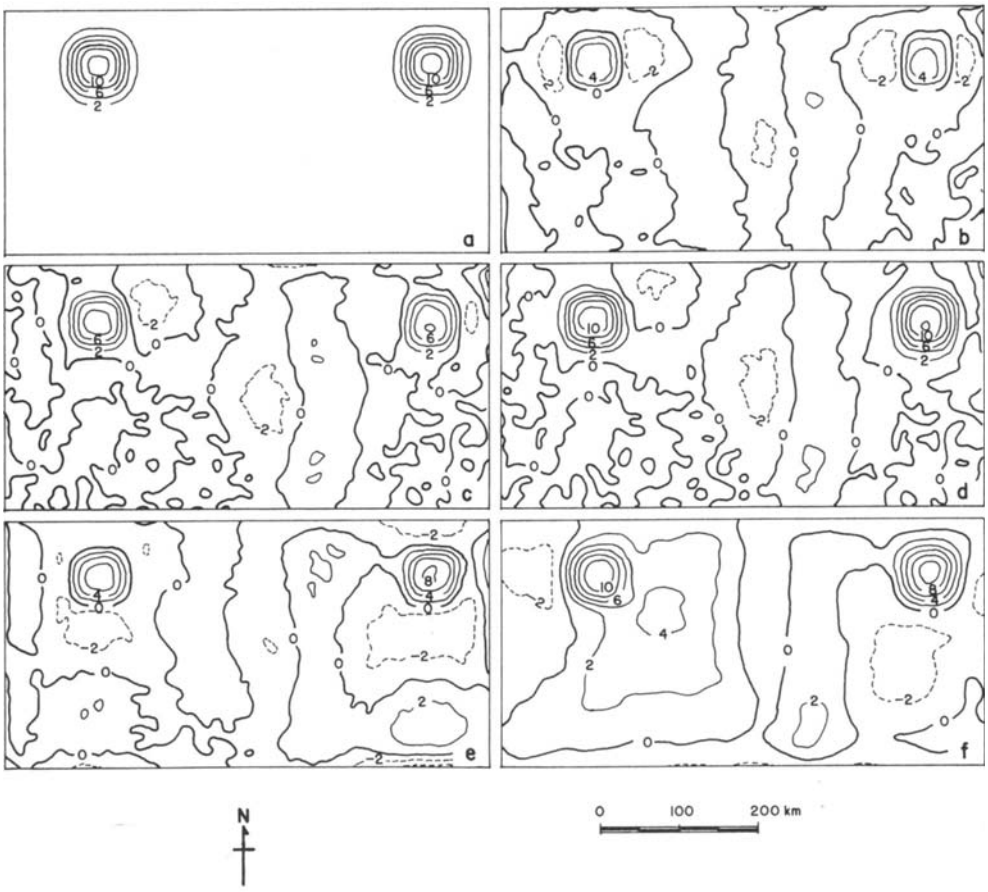

FIG. 5. Comparison among residuals obtained by subtracting the different regionals shown in Figure 4 from the total field (Figure 4a). (a) Theoretical residual, (b) least-squares, (c) PW, (d) PNW, (e) orthogonal polynomials of orders 4 (north-south) and 9 (east-west), and (f) spectral method. Dashed lines indicate negative anomalies. Contour interval is 2 mGal.

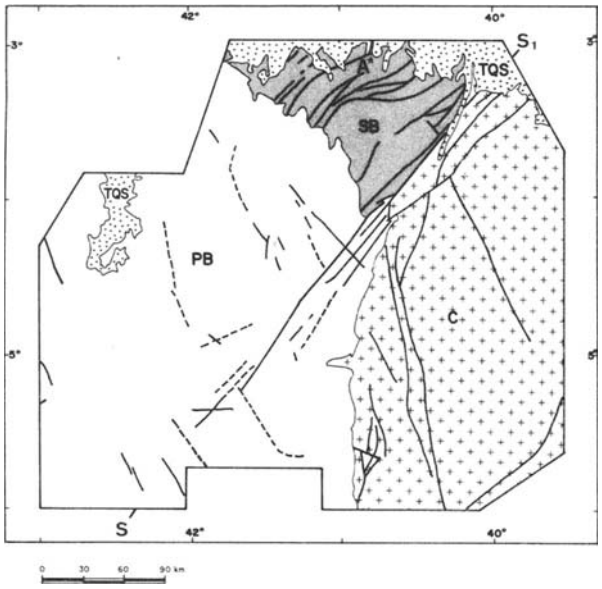

FIG. 6. Map showing the main structural and tectonic features in Ceará State, Brazil. A shear belt (SB) bounds two cratonic blocks, one on the southeast (C) and another on the northwest (not shown). The cratonic block on the northwest is overlain by Paleozoic and Mesozoic sediments from the Parnaíba Basin (PB). TQS are Tertiary and Quaternary sediments. Thick solid lines are mapped faults, and dashed lines are faults inferred from field work and aerophotographic interpretation.

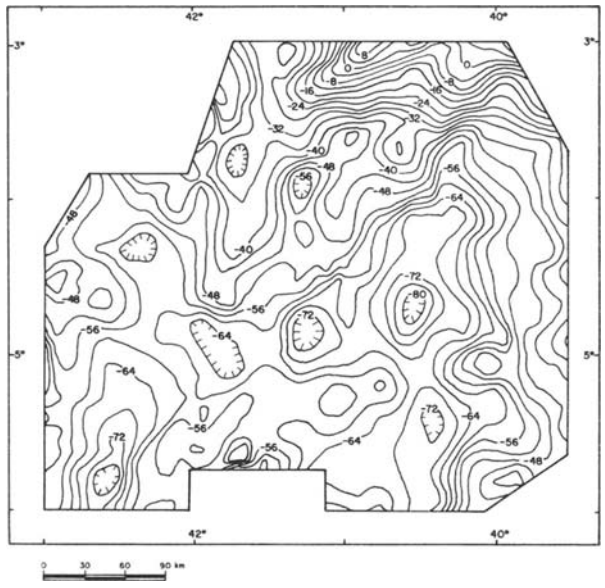

FIG. 7. Bouguer gravity anomaly map of the Ceará State. Contour interval 4 mGal. Hachures indicate gravity lows.

over, the computed positive residual anomalies are too narrow in both the north-south and east-west directions as compared to the theoretical anomaly.

The PW method (Figure 5c) shows an improvement in the computed residual amplitudes, but they are still one half of the true amplitude. Spurious, negative anomalies are present but more limited, in contrast with least-squares. The PNW method (Figure 5d), however, produces the best computed residual. The amplitudes, gradients and widths of both residual anomalies are very close to the true values. In addition, the spurious negative anomalies are either absent or distant from the positive anomalies.

Figure 5e shows the residual corresponding to the regional obtained by fitting an orthogonal polynomial of orders 4 and 9 in the north-south and east-west directions, respectively. There is an improvement in the computed amplitudes and widths of the residual anomalies with respect to least squares. However, pronounced spurious negative and positive anomalies in the north-south direction, particularly in the eastern portion, are present and are probably due to the insufficient polynomial order along the north-south direction.

Figure 5f displays the residual obtained by Syberg's spectral method. The amplitudes, gradients, and widths of the computed residual anomalies are in good agreement with the theoretical values, although not as good as the PNW method. There are, however, large spurious negative anomalies around the main positive residual anomalies. Moreover, the presence of large spurious positive anomalies distorts the map further. These positive anomalies are clearly associated with the regional field which was incorporated to the computed residual field in this case. The spectral overlap of both fields prevented a clearcut separation by the spectral method.

APPLICATION TO REAL DATA

Geologic setting

The survey area lies in the Ceará State, Brazil, along the northwestern border of a cratonic area consisting of gneisses, granitoids, and supracrustal rocks interpreted as a greenstone belt (area labeled C in Figure 6). On the northwest, this area is bounded by the Northwest Ceará shear belt comprised of gneisses, granulites, granitoids, and supracrustal rocks (Abreu et al., 1988). The orientation in the shear belt is essentially northeast-southwest, and right-lateral fault predominate. Close to point A (Figure 6) the presence of outcropping granulitic rocks preserved in the middle of migmatized gneisses is interpreted as resulting from an overthrust of the eastern block (containing the greenstone belt) onto the western block which is overlain by the sediments of the Parnaíba Basin. During this process, the granulitic rocks are raised from the lower crust to shallow levels and are partly retrometamorphosed (Gorayeb and Abreu, 1989). Because these shallow, dense, high-grade metamorphic rocks usually do not outcrop, their presence can be detected only indirectly, by gravimetry.

Gravity data

A total of 1220 gravity observations were collected along the existing roads using a LaCoste and Romberg gravity

meter. About 20 percent of the stations were located at benchmarks and 73 percent were positioned at mapped roads with the help of the vehicle odometer. The remaining 7 percent were located on unmapped roads and positioned with the help of a compass and the vehicle odometer. The precision in the altitude determination is better than 5 cm for the stations located at the benchmarks and 2 m for the remaining ones, where the altitude was obtained with an altimeter. The horizontal positioning of the stations not located at benchmarks has an imprecision of about 90 m. Gravity coverage is fairly uniform; spacing between stations varies from 1 km to 17 km with an average of 8 km. The data were corrected for the effect of latitude using the 1930 International formula (Nettleton, 1976) and reduced to the sea level by combined elevation correction. A density of 2500 kg/m^3 was employed in this correction for stations at the top of the sedimentary rocks and 2670 kg/m^3 for the remaining stations. The uncertainties in determining the horizontal and vertical positioning produce maximum errors of 0.02 and 0.41 mGal in the latitude and combined elevation corrections, respectively. The data were not terrain corrected because the topography is essentially smooth except for a 600 m cliff in the middle of the area. The resulting data were gridded at a regular 7.5 km grid spacing both in the north-south and east-west directions using La Porte's (1962) method. The reduced data were contoured by computer to produce the Bouguer anomaly map (Figure 7).

Regional-residual separation

The geologic and tectonic model of the area assumes the occurrence of dense granulitic masses in the upper crust, raised from the lower crust by a compressive event. A regional-residual separation applied to the gravity data is expected to isolate the residual anomalies produced by the shallow granulitic bodies from regional anomalies, possibly

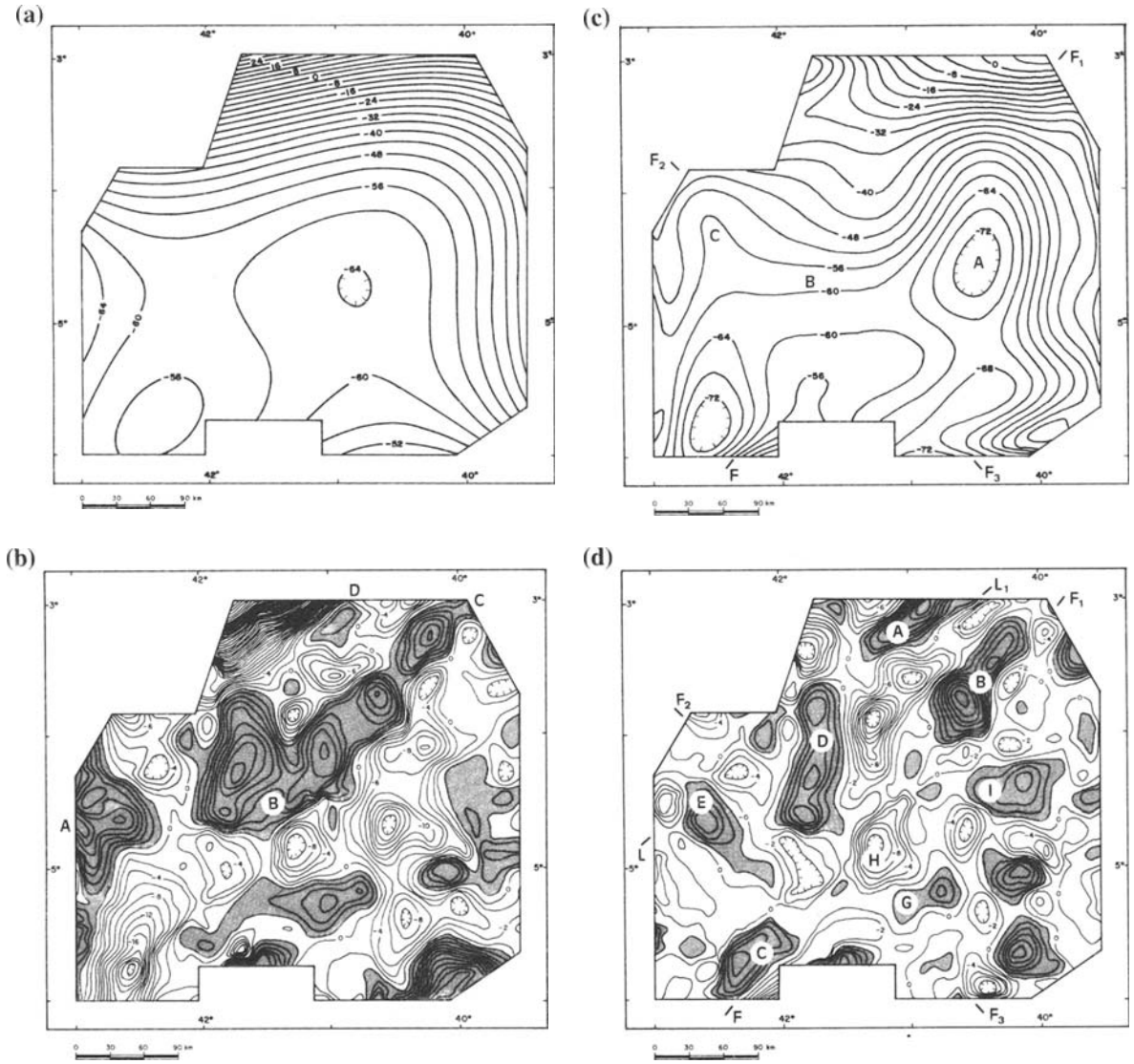

FIG. 8. Third-order regional (a) and residual (b), and ninth-order regional (c) and residual (d) anomaly maps from the Ceará State area using the PNW method. Positive residual anomalies greater than 2 mGal are shaded and the contour intervals are 4 mGal for the regionals and 2 mGal for the residuals. Hachures point downslope on contours enclosing closed lows.

produced by irregularities (caused by the compressive event) at the crust-mantle interface.

The proposed PNW method was applied to the gravity data of Figure 7 for polynomials of orders 3 and 9. The fitted surface of order 3 (Figure 8a) shows a large low anomaly at the southeastern quadrant and a very steep positive gradient toward the northern border. The corresponding residual map (Figure 8b) shows an arcuate strip of highs (ABC in Figure 8b) and a significant high at the southeastern corner. At point D, where granulites outcrop and a strong positive anomaly was expected, there is a modest high. The residual field in general does not provide much insight on the subsurface geology, except for the linear segment BC which coincides with the surface expression of a mapped fault crossing the area (SS_1 in Figure 6). The gravity highs are probably related to granulites in subsurface along this fault. This example supports the conclusion, obtained from analysis of theoretical models, that a polynomial surface of order 3 is generally insufficient to approximate even the gross features of a regional field.

On the other hand, the major regional features represented by the surface of order 9 (Figure 8c) are consistent with the known tectonic evolution of the area. The predominant low (A in Figure 8c), for example, may be due to a crustal thickening in the southeastern block along FF_1. This thickening possibly formed from compression and overthrusting of the southeastern block onto the northwestern block. The north-northeast strike of this low is interrupted by an east-west feature (B in Figure 8c) which extends westward to a northwest-southeast low (C). These lows may be related to another fault at F_2F_3, possibly associated with compressive stress deep in the lower crust, according to models presented by Beltrão (1989).

The corresponding residual field (Figure 8d) shows the presence of linear, high-gradient, positive anomalies in the north, northwest, and southwest, and rounded, low to moderate gradient, positive anomalies in the east and southeast. These two areas are separated by the major northeast-southwest fault FF_1 which coincides with the surface expression of the mapped SS_1 fault in Figure 6. Linear anomaly A is related to outcropping granulites, and anomalies B and C are probably due to the presence of granulites in subsurface. This gravity interpretation led to a detailed field survey near anomaly B where outcrops of granulite were subsequently found. The positive residual anomalies (A, B, and C) are parallel to the general lineaments of the shear belt where the granulites are either thrusted from the lower crust or resulted from metamorphism of rocks submitted to extreme conditions of pressure and temperature. Anomaly D is similar to anomalies A, B, and C, but its strike is different, suggesting that its southern end, once contiguous to anomaly E, was offset by a right-lateral fault at F_2F_3. The same fault may have displaced anomaly G from its original position now occupied by the low H.

CONCLUSIONS

We present a new, automatic regional-residual separation method for gravity data which fits a polynomial surface to the data using a robust procedure instead of the least-squares criterion. The method lessens the residual influence in the fitted regional by assuming that isolated anomalies are locally either positive or negative (but not both).

Using synthetic data, we obtained residuals having amplitude, gradient, and horizontal extent closer to the true values than those produced by the least-squares method. Also, the regional can be approximated by a high-order polynomial without incorporating part of the residual. The fitted regional is, therefore, closer to the true regional while the regional obtained by the least-squares method, being limited to a low-order polynomial surface to prevent the residual transmission, is more distorted. The proposed method has also a superior performance as compared with spectral methods. Spectral methods cannot address the regional and residual spectra overlap. Traditional polynomial fitting, being equivalent to a low-pass filtering operation, has the same difficulty. The proposed method is less sensitive to the limitation imposed by the spectral overlap to regional-residual separation because it employs a priori information which is independent of the spectrum, namely, that an isolated gravity anomaly due to a single body has values of the same sign.

The application of the proposed method to real data produced geologically meaningful regional and residual fields, whose interpretation contributed to the understanding of the tectonic development of the area.

ACKNOWLEDGMENTS

We thank Jorge W. D. Leão for critically reading the manuscript, João B. S. Costa for helpful discussions and assistance regarding the tectonic evolution of the area under investigation, and the reviewers of the manuscript for their suggestions. Financial support for this research was provided by Conselho Nacional de Desenvolvimento Científico e Tecnológico (CNPq) and Financiadora de Estudos e Projetos (FINEP), Brazil. The field work was supported by the International Cooperation Program CNPq-CNRS (Centre National de la Recherche Scientifique, France).

REFERENCES

Abdelrahman, E. M., Riad, S., Refai, E., and Amin, Y., 1985, On the least-squares residual anomaly determination: Geophysics, **50**, 473–480.

Abreu, F. A. M., Gama Jr., T., Gorayeb, P. S. S., and Hasui, Y., 1988, O cinturão de cisalhamento Noroeste do Ceará. Anais do VII Cong. Latino-Americano de Geologia, Belém, 20–34.

Agocs, W. B., 1951, Least-squares residual anomaly determination: Geophysics, **16**, 686–696.

Anderson, K. R., 1982, Robust earthquake location using M-estimates: Phys. Earth Plan. Int., **30**, 119–130.

Beltrão, J. F., 1989, Uma nova abordagem para interpretação de ano malias gravimétricas regionais e residuais aplicada ao estudo da organização crustal—Exemplo da região Norte do Piauí e Noroeste do Ceará: Dr. dissertation, Fed. Univ. of Pará, Brazil.

Browne, S. E., Fairhead, J. D., and Mohamed, I. I., 1985, Gravity study of the White Nile Rift, Sudan, and its regional tectonic setting: Tectonophys., **113**, 123–137.

El-Batroukh, S. I., and Zentani, A. S., 1980, Gravity interpretation of Raguba field, Sirte basin, Libya: Geophysics, **45**, 1153–1163.

Galson, D. A., and Mueller, St., 1986, An introduction to the European geotraverse project: first results and present plans: Tectonophys., **126**, 1–30.

Gorayeb, P. S. S., and Abreu, F. A. M., 1989, A faixa de alto grau da região de Cariré—CE. Atas do II Simpósio Nacional de Estudos Tectônicos, Fortaleza. SBG. Núcleos Fortaleza, Nordeste e Bahia. 261–264.

Gol'tsman, F. M., 1977, Problems of the statistical information theory of the interpretation of geophysical observations: Physics of the Solid Earth, **13**, 873–879.

Gupta, V. K., and Ramani, N., 1980, Some aspects of regional-residual separation of gravity anomalies in a Precambrian terrain: Geophysics, **45**, 1412–1426.

Huber, P. J., 1981, Robust statistics: John Wiley and Sons.
Jacobsen, B. H., 1987, A case for upward continuation as a standard separation filter for potential-field maps: Geophysics, **52**, 1138–1148.
La Porte, M., 1962, Elaboration rapide de cartes gravimetriques deduites de l'anomalie de Bouguer a l'aide d'une calculatrice electronique: Geophys. Prosp., **10**, 238–257.
Nettleton, L. L., 1976, Gravity and magnetics in oil prospecting: McGraw-Hill Book Co.
Paul, M. K., 1967, A method of computing residual anomalies from Bouguer gravity map by applying relaxation technique: Geophysics, **32**, 708–719.
Ralston, A., and Rabinowitz, P., 1978, A first course in numerical analysis: McGraw-Hill Book Co.
Rao, B. S. R., Radhakrishna Murthy, I. V., and Visweswara Rao, C., 1975, A successive approximation method of deriving residual gravity: Geoexpl., **13**, 129–135.
Ritz, M., and Robineau, B., 1986, Crustal and upper mantle electrical conductivity structures in West Africa: geodynamic implications: Tectonophys., **124**, 115–132.
Simpson, S. M., Jr., 1954, Least-squares polynomial fitting to gravitational data and density plotting by digital computers: Geophysics, **19**, 255–269.
Skeels, D. C., 1967, What is residual gravity?: Geophysics, **32**, 872–876.
Syberg, F. J. R., 1972, A Fourier method for the regional-residual problem of potential fields: Geophys. Prosp., **20**, 47–75.
Tukey, J. W., 1965, Data analysis and the frontiers of geophysics: Science, **148**, 1283–1289.
Ulrych, T. J., 1968, Effect of wavelength filtering on the shape of the residual anomaly: Geophysics, **33**, 1015–1018.